

5-1-2016

Interactive Effects of Physical Activity and APOE- $\epsilon 4$ On White Matter Tract Diffusivity in Healthy Elders

J. Carson Smith

University of Maryland, College Park

Melissa A. Lancaster

Rosalind Franklin University of Medicine and Science

Kristy A. Nielson

Marquette University, kristy.nielson@marquette.edu

John L. Woodard

Wayne State University

Michael Seidenberg

Rosalind Franklin University of Medicine and Science

See next page for additional authors

Accepted version. *NeuroImage*, Vol. 131 (May 1, 2016): 102-112. [DOI](#). © 2015 Elsevier Inc. Used with permission.

NOTICE: this is the author's version of a work that was accepted for publication in *NeuroImage*. Changes resulting from the publishing process, such as peer review, editing, corrections, structural formatting, and other quality control mechanisms may not be reflected in this document. Changes may have been made to this work since it was submitted for publication. A definitive version was subsequently published in *NeuroImage*, Vol. 131 (May 1, 2016): 102-112. [DOI](#)

Authors

J. Carson Smith, Melissa A. Lancaster, Kristy A. Nielson, John L. Woodard, Michael Seidenberg, Sally Durgerian, Ken Sakaie, and Stephen M. Rao

Interactive Effects of Physical Activity and *APOE-ε4* On White Matter Tract Diffusivity in Healthy Elders

J. Carson Smith

Department of Kinesiology, School of Public Health, University of Maryland, College Park, MD

Melissa A. Lancaster

Department of Psychology, Rosalind Franklin University of Medicine and Science, North Chicago, IL

Department of Neurology, Medical College of Wisconsin, Milwaukee, WI

Kristy A. Nielson

Department of Neurology, Medical College of Wisconsin, Milwaukee, WI

Department of Psychology, Marquette University, Milwaukee, WI

John L. Woodard

Department of Psychology, Wayne State University, Detroit, MI

Michael Seidenberg

*Department of Psychology,
Rosalind Franklin University of Medicine and Science,
North Chicago, IL*

Sally Durgerian

*Department of Neurology, Medical College of Wisconsin,
Milwaukee, WI*

Ken Sakaie

*Imaging Institute, Cleveland Clinic,
Cleveland, OH*

Stephen M. Rao

*Schey Center for Cognitive Neuroimaging, Neurological Institute,
Cleveland Clinic,
Cleveland, OH*

Abstract: Older adult apolipoprotein-E epsilon 4 (*APOE-ε4*) allele carriers vary considerably in the expression of clinical symptoms of Alzheimer's disease (AD), suggesting that lifestyle or other factors may offer protection from AD-related neurodegeneration. We recently reported that physically active *APOE-ε4* allele carriers exhibit a stable cognitive trajectory and protection from hippocampal atrophy over 18 months compared to sedentary *ε4* allele carriers. The aim of this study was to examine the interactions between genetic risk for AD and physical activity (PA) on white matter (WM) tract integrity, using diffusion tensor imaging (DTI) MRI, in this cohort of healthy older adults (ages of 65 to 89). Four groups were compared based on the presence or absence of an *APOE-ε4* allele (High Risk; Low Risk) and self-reported frequency and intensity of leisure time physical activity (PA) (High PA; Low PA). As predicted, greater levels of PA were associated with greater fractional anisotropy (FA) and lower radial diffusivity in healthy older adults who did not possess the *APOE-ε4* allele. However, the effects of PA were reversed in older adults who were at increased genetic risk for AD, resulting in significant interactions between PA and genetic risk in several WM tracts. In the High Risk-Low PA participants, who had exhibited episodic memory decline over the previous 18-months, radial diffusivity was lower and fractional anisotropy was higher, compared to the High Risk-High PA participants. In WM tracts that subserve learning and memory processes, radial diffusivity (DR) was negatively correlated with episodic memory performance in physically inactive *APOE-ε4* carriers, whereas DR was

positively correlated with episodic memory performance in physically active *APOE-ε4* carriers and the two Low Risk groups. The common model of demyelination-induced increase in radial diffusivity cannot directly explain these results. Rather, we hypothesize that PA may protect *APOE-ε4* allele carriers from selective neurodegeneration of individual fiber populations at locations of crossing fibers within projection and association WM fiber tracts.

Keywords: Alzheimer's disease, Cognitive aging, Diffusion tensor imaging, Exercise, Genetic risk, Radial diffusivity, Physical activity, White matter integrity

Introduction

The apolipoprotein-E epsilon4 (*APOE-ε4*) allele is the only clearly identified candidate gene for late-onset Alzheimer's disease (AD). However, it is an imperfect predictor of who will develop clinical symptoms of the disease (Bird, 2008). The variability in clinical manifestation of AD among *APOE-ε4* allele carriers suggests that other factors may offer protection from AD-related neurodegeneration and that interventions aimed at slowing or reversing AD-related processes may be effective if initiated at a much earlier stage of disease progression (Sperling et al., 2014). Identification of preclinical biomarkers that reflect increased risk from the *APOE-ε4* allele may permit better prediction of future cognitive decline and development of targeted interventions (Bateman et al., 2012, Clark et al., 2008, Reiman et al., 2010 and Woodard et al., 2010). Physical activity (PA), in both cross sectional and prospective studies, has been shown to protect healthy older adults against cognitive decline (Barnes and Yaffe, 2011 and Etgen et al., 2010) and dementia onset (Beckett et al., 2015) and have beneficial effects on brain structure (Erickson et al., 2011) and function (Colcombe et al., 2004 and Smith et al., 2013). PA has been shown to have a particularly strong protective effect among healthy older adult *ε4* allele carriers, compared to non-carriers, in the maintenance of hippocampal volume (Smith et al., 2014) and cognitive function (Schuit et al., 2001 and Woodard et al., 2012), protection against the accumulation of brain amyloid (Head et al., 2012), and enhancement of semantic memory network activation measured by fMRI (Smith et al., 2011). However, the neurophysiological mechanisms associated with the neuroprotective effects of PA in *APOE-ε4* allele carriers have not been clearly defined.

The *APOE-ε4* allele is associated with several biochemical processes that have been implicated in the etiology of AD (i.e., amyloid deposits, neurofibrillary tangle formation, neuronal cell death, oxidative stress, neuroinflammation, synaptic alterations, and cholinergic signaling dysfunction; Lane and Farlow, 2005 and Poirier, 2000). White matter fiber tract integrity, as measured by diffusion tensor imaging (DTI), is a biomarker that has been shown to be compromised in AD and MCI patients. Individuals diagnosed with mild cognitive impairment and AD exhibit greater isotropic patterns of water diffusivity (i.e., lower fractional anisotropy (FA); greater mean (MD), axial (DA), and radial (DR) diffusivity) that may reflect disease-related neurodegenerative processes within neural networks (Bosch et al., 2012). In comparison, very few differences have been reported between healthy cognitively intact *APOE-ε4* allele carriers and non-carriers using DTI indices of white matter integrity (Gold et al., 2010 and Nyberg and Salami, 2014). The absence of large-scale differences may result from the potential moderating role of PA, which was not taken into consideration in these studies.

Greater levels of PA have been associated with greater FA and lower MD within select AD-relevant fiber tracts in healthy older adults (Johnson et al., 2012, Marks et al., 2011, Tian et al., 2014a and Tseng et al., 2013). However, the size of these effects have been relatively small and reported in only a few selected tracts, perhaps because DTI studies assessing the effects of PA did not consider genetic risk for AD as a moderating variable. The possible differential effect of PA on DTI measures of white matter fiber tract integrity in healthy older adult *APOE-ε4* allele carriers and non-carriers has not been reported.

We recently published a series of papers that have examined the moderating effect of PA on indices of brain structure and brain function based on a cohort of healthy older adults who participated in a 5-year longitudinal observational study (Rao et al., 2015). We previously reported that over an 18-month period, greater levels of PA in *APOE-ε4* allele carriers significantly reduced the risk for cognitive decline (Woodard et al., 2012) and preserved hippocampal volume (Smith et al., 2014) compared to physically inactive carriers. Moreover, we found that physically active *APOE-ε4* allele carriers showed a greater intensity of brain activation during a semantic memory task. This increased activation also predicted stability of

cognitive function over 18 months in this cohort (Woodard et al., 2010). In the current study, we examined the interactive effects of two levels of PA participation and the presence or absence of the *APOE-ε4* allele on DTI indices of white matter tract integrity. These DTI data were not available at baseline but were collected 18 months after baseline, when a disproportionately greater proportion of physically inactive *APOE-ε4* allele carriers had experienced cognitive decline and hippocampal atrophy relative to physically active carriers. Based on the previous literature, we hypothesized that greater PA would be related to greater FA and lower rates of radial water diffusion in white matter tracts, and that greater genetic risk would be associated with lower FA and greater rates of radial water diffusion. Furthermore, we hypothesized that these main effects of PA and genetic risk would be secondary to significant interactions between genetic risk and PA, such that PA would benefit *APOE-ε4* allele carriers more than *APOE-ε4* allele non-carriers.

Method

Participants

Healthy adults between the ages of 65 and 89 were recruited from newspaper advertisements. A telephone screen was administered initially to 459 individuals to determine eligibility based on inclusion/exclusion criteria. Potential participants were excluded if they reported a history of cognitive deterioration and/or dementia, neurological disease (cerebral ischemia, vascular headache, carotid artery disease, cerebral palsy, epilepsy, brain tumor, chronic meningitis, multiple sclerosis, pernicious anemia, normal-pressure hydrocephalus, HIV infection, Parkinson's disease, and Huntington's disease), medical illnesses (untreated hypertension, glaucoma, and chronic obstructive pulmonary disease), major psychiatric disturbance or substance abuse generally consistent with DSM-IV Axis I criteria or a Geriatric Depression Scale (GDS) score greater than 15. Participants were allowed to take cardiovascular drugs.

To enrich the sample with a higher percentage of *APOE-ε4* carriers, half the sample was recruited based on a family history of dementia because the *APOE-ε4* allele is more common in individuals

with a family history of dementia than among those without such a history (Sager et al., 2005). Family history was defined as a report of a clear clinical diagnosis of AD or a reported history of gradual decline in memory and other cognitive functions, confusion, or judgment problems without a formal diagnosis of AD prior to death in a first-degree relative. As expected, a family history of AD was more common in *APOE-ε4* allele carriers ($n = 24$; 70.6%) than non-carriers ($n = 25$; 46.3%) (chi-square = 4.99; $p = .026$).

Of those who met criteria, 99 completed testing at the 18-month follow-up (when the current DTI pulse sequence was initiated) and had agreed to undergo *APOE* genotyping from blood samples, complete a PA questionnaire, be administered a brief neuropsychological and behavioral assessment, and undergo a magnetic resonance imaging (MRI) scan session. Diffusion tensor and structural MRI scans were available from 88 of 99 (88.9%) participants. DTI data from six participants were not collected due to time constraints or the participants' desire to end the scan session; data from three participants were lost due to technical errors and data corruption; one participant (Low Risk-High PA group) was excluded as an outlier; and one participant did not undergo the MRI scan session. From the final pool of 88 participants (87 Caucasian, 1 African American), four subgroups were formed based on the absence/presence of one or both *APOE-ε4* alleles (Low Risk vs. High Risk) and self-reported frequency of leisure time PA (Low PA vs. High PA).

This study was approved by the institutional review board at the Medical College of Wisconsin and conducted in accordance with the Helsinki Declaration. Written informed consent was obtained and all participants received modest financial compensation.

Physical activity

Frequency and intensity of leisure time PA were measured using the Stanford Brief Activity Survey (SBAS) (Taylor-Piliae et al., 2006). There is good evidence for the reliability and validity of SBAS scores to assess habitual PA in adults and older adults. (Taylor-Piliae et al., 2010, Taylor-Piliae et al., 2007 and Taylor-Piliae et al., 2006). For moderate intensity PA, the SBAS had a sensitivity of 0.73 and a

specificity of 0.61 (Taylor-Piliae et al., 2006). Participants who endorsed one of the two items indicating two or fewer days of low intensity PA (ranging from no PA to slow walking or light chores) were classified as physically inactive (Low PA). Participants endorsing one of the remaining three items describing moderate to vigorous intensity PA three or more days per week (ranging from brisk walking, jogging or swimming for 15 min or more, or moderately difficult chores for 45 min, to regular jogging, running, bicycling or swimming for 30 min or more, or playing sports such as handball or tennis for an hour or more) were classified as physically active (High PA) (Smith et al., 2011, Smith et al., 2014 and Woodard et al., 2012).

Genetic testing

APOE genotype was determined using a polymerase chain reaction method (Saunders et al., 1996). Deoxyribonucleic acid was isolated with Genra Systems Autopure LS for Large Sample Nucleic Acid Purification. Participants with one or both APOE- ϵ 4 alleles were classified as High Risk for developing AD and the remainder classified as Low Risk. APOE genotype results for the four groups were as follows: Low Risk-High PA ($n = 21$: 3 ϵ 2/ ϵ 3 and 18 ϵ 3/ ϵ 3), Low Risk-Low PA ($n = 33$: 5 ϵ 2/ ϵ 3 and 28 ϵ 3/ ϵ 3), High Risk-High PA ($n = 20$: 18 ϵ 3/ ϵ 4 and 2 ϵ 4/ ϵ 4), and High Risk-Low PA ($n = 14$: 1 ϵ 2/ ϵ 4 and 13 ϵ 3/ ϵ 4).

Neuropsychological testing

Cognitive functioning was determined from a neuropsychological test battery (Woodard et al., 2009) consisting of the Mini-Mental State Examination (MMSE; Folstein et al., 1975), Mattis Dementia Rating Scale, 2nd Edition (DRS-2; Jurica et al., 2001), and the Rey Auditory Verbal Learning Test (RAVLT; Rey, 1958), measures commonly used to assess general cognitive status and anterograde memory impairment. In addition, the Geriatric Depression Scale (GDS) (Yesavage, 1988) and Lawton Activities of Daily Living (ADL) scale (Lawton and Brody, 1969) were both administered along with the neuropsychological assessments.

Data collection

Participants underwent reviews of their medical and psychosocial history, completed the neuropsychological test battery (MMSE, DRS-2, RAVLT, GDS, ADL), and underwent functional and structural MRI scanning at baseline and 18 months. Only data from the 18-month follow-up are reported here since the DTI scans were collected only during this examination. We incorporated the baseline neuropsychological testing to calculate the number of participants who experienced a significant cognitive decline over the previous 18-month follow-up (for details, see Woodard et al., 2012).

Structural image acquisition

DTI and high-resolution anatomical images were collected on a General Electric (Waukesha, WI) Signa Excite 3.0 T short bore scanner at Froedtert Hospital (Milwaukee, WI). Foam padding was used to reduce head movement within the coil. High-resolution anatomical scans were obtained from a three-dimensional spoiled gradient-recalled at steady-state (SPGR) pulse sequence (TE = 3.9 ms; TR = 9.5 ms; inversion recovery (IR) preparation time = 450 ms; flip angle = 12°; number of excitations (NEX) = 2; slice thickness = 1.0 mm; field of view (FOV) = 24 cm; resolution = 256 × 224; slices = 144).

Diffusion tensor imaging

Whole brain (35 axial slices; 4 mm) diffusion tensor images were acquired with 25 encoding directions ($b = 1000 \text{ s/mm}^2$; TE = min (86.5 ms); TR = 10,000 ms; FOV = 240 mm, matrix = 128 × 128; acquisitions = 1). Images were smoothed at 6 mm FWHM to eliminate Gibbs ringing. Head movement and eddy currents were corrected and the Brain Extraction Tool (BET; Smith, 2002) was applied to exclude non-brain voxels. Each diffusion-weighted image was registered to the corresponding b0 image (no diffusion encoding). Fractional anisotropy (FA), mean diffusivity (MD), axial diffusivity (DA), and radial diffusivity (DR) images were created by fitting a tensor model to the raw diffusion data using the FSL Diffusion Toolbox (Behrens et al., 2003).

DTI processing methods

DTI data were first processed using the Tract-Based Spatial Statistics (TBSS Smith et al., 2006) program found in FSL 4.0 image processing software (<http://www.fmrib.ox.ac.uk/fsl/tbss/index.html>) to create a mean white matter skeleton. Specifically, all FA images were aligned to the FMRIB58 standard image in cubic 1 mm standard space. FA images were averaged and a skeleton created with an FA threshold of 0.2 representing tracts common to all participants. This method of "thinning" each white matter tract perpendicular to the tract and applying a threshold for FA helps to eliminate the threat of partial volume effects and areas of high inter-subject variability (Smith et al., 2006). Each participant's maximum FA value from the nearest relevant tract center was assigned to the corresponding skeleton voxel, which corrects for residual misalignments after nonlinear registration. Diffusivity measures from the same maximum FA voxels were also assigned to the corresponding skeleton voxels.

Following the creation of the FA skeleton, white matter tracts of interest were created using the ICBM DTI-81 white matter atlas (Mori et al., 2008). The atlas consists of 48 white matter tracts based on acceptable levels of intra- and inter-rater reliability. Using the Analysis of Functional NeuroImages (AFNI) software package (Cox, 1996), the TBSS-derived FA skeleton was overlaid onto the ICBM DTI-81 atlas. From this conjunction map, mean FA, MD, DA, and DR values were calculated for each subject for each of 25 white matter tracts of interest. Fig. 1 shows the 25 tracts of interest investigated as represented in the ICBM DTI-81 atlas. Data were screened and outliers greater than three standard deviations from the mean were removed (< 1% of data).

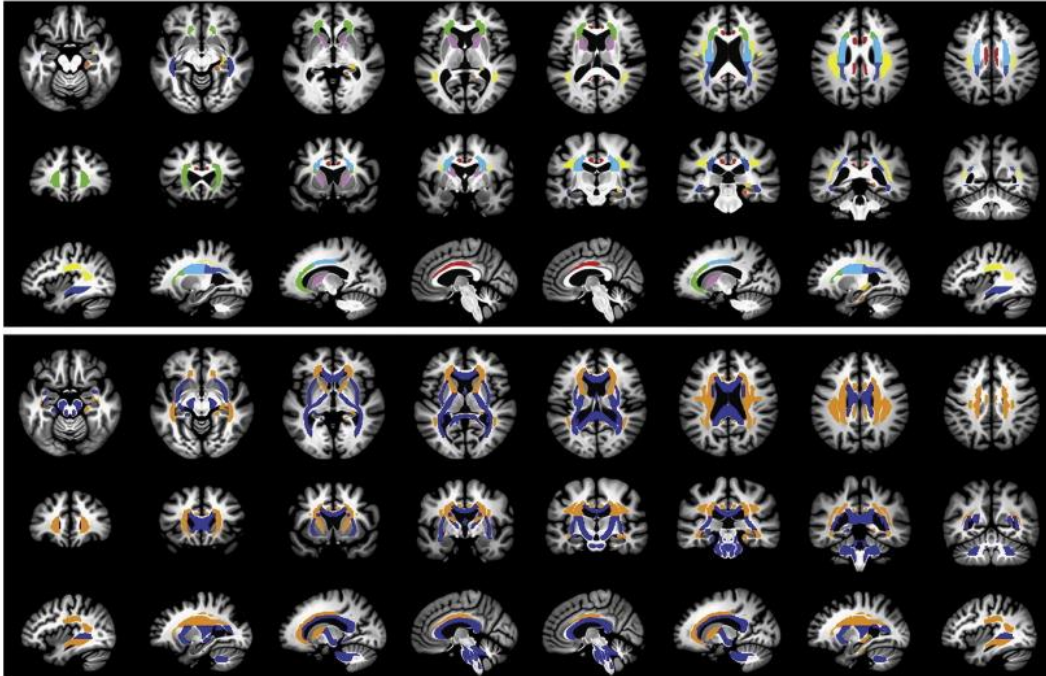


Fig. 1. (Top) Axial (inferior to superior from left to right), coronal (rostral to caudal from left to right), and sagittal (left hemisphere to right hemisphere from left to right) views of the white matter fiber tract mask that was created, from which the DTI data were extracted and compared in the statistical analysis. The colors of each tract represent each of the bilateral or midline fiber tracts of interest based on the ICBM DTI-81 white matter atlas (Mori et al., 2008); anatomical labels for the tracts are listed in Table 2. (Bottom) Axial (inferior to superior from left to right), coronal (rostral to caudal from left to right), and sagittal (left hemisphere to right hemisphere from left to right) views of the significant interactions between genetic risk and physical activity for radial diffusivity, shown in orange. White matter tracts with non-significant interaction effects for radial diffusivity are shown in blue.

Statistical analysis

FA, MD, DA, and DR values from each WM tract were subjected to a 2 (High Risk vs. Low Risk) \times 2 (High PA vs. Low PA) analysis of variance (ANOVA; SPSS 21, Chicago, IL), with age at the time of the scan as a covariate. Significant effects were followed by post-hoc group comparisons with the false discovery rate (FDR) threshold used to control the family-wise error rate with significance at $p < .05$.

Results

Participant characteristics and cognitive status

Demographic characteristics, neuropsychological test scores, cognitive trajectory over the past 18 months, symptoms of depression, and activities of daily living are presented for the four participant groups (Low Risk-High PA, $n = 21$; Low Risk-Low PA, $n = 33$; High Risk-High PA, $n = 20$; High Risk-Low PA, $n = 14$) in Table 1. The groups were not significantly different in age, education, or sex, and were similar in symptoms of depression and activities of daily living. As reported in our prior work (Woodard et al., 2010 and Woodard et al., 2012), all participants were determined to be cognitively intact at the baseline assessment conducted 18 months prior to the data presented in the current study. As reported in our prior publications (Woodard et al., 2010 and Woodard et al., 2012), the High Risk-Low PA group had a greater proportion of participants who declined by more than 1 SD on either the RAVLT immediate recall, RAVLT delayed recall or the DRS total score compared to the High Risk-High PA group and high and low PA non-carriers.

Table 1. Participant Characteristics (mean \pm SD; $n = 88$) and summary result of the 2 (Risk) \times 2 (PA) between-groups ANOVAs.

Variables	Low risk		High risk		Interaction p	Interaction η_p^2
	High PA ($n = 21$)	Low PA ($n = 33$)	High PA ($n = 20$)	Low PA ($n = 14$)		
<i>Demographics</i>						
Age (yrs)	76.0 (4.7)	73.5 (4.7)	73.1 (4.4)	74.0 (4.2)	0.10	0.03
Education (yrs)	14.8 (2.7)	14.0 (2.0)	15.4 (3.2)	15.6 (3.1)	0.45	<0.01
Sex	6M, 15F	7M, 26F	5M, 15F	5M, 9F	0.37	0.01
<i>Neuropsychological testing</i>						
MMSE	29.5 (0.9)	29.6 (1.0)	29.4 (1.1)	28.7 (1.1)	0.10	0.03
DRS total	138.1 (2.6)	139.2 (2.1)	137.1 (4.0)	137.8 (3.7)	0.72	<0.01
AVLT trials 1-5	46.1 (6.4)	48.9 (7.3) ^a	46.2 (8.5)	41.6 (8.9) ^a	0.04	0.05
AVLT IR	9.2 (2.1)	10.2 (2.6) ^a	9.4 (3.2) ^a	7.2 (2.7) ^{ab}	0.01	0.08
AVLT DR	9.0 (2.5) ^a	10.0 (2.9) ^a	8.8 (3.4) ^a	6.1 (2.6) ^{abc}	0.01	0.09
<i>Prior 18-month cognitive trajectory</i>						
Declined > 1 SD (#, %)	6, 28	6, 24	6, 30	11, 79	<0.01	
<i>Depression symptoms and activities of daily living</i>						
GDS	1.8 (2.4)	2.5 (2.5)	3.0 (2.5)	1.7 (2.7)	0.07	0.04
Lawton ADL	5.0 (0.0)	4.9 (0.2)	4.9 (0.3)	4.9 (0.3)	0.53	<0.01

Notes: All neuropsychological indices represent raw scores. Common superscript within each variable indicates significant differences between groups ($p < .05$, FDR-corrected); ^b = $p < .05$, but does not survive FDR threshold for significance. High

Risk = APOE-ε4 allele carrier; PA = physical activity; M = male; F = female; MMSE = Mini-Mental State Exam; DRS = Mattis Dementia Rating Scale; AVLT = Rey Auditory Verbal Learning Test; DR = delayed recall; GDS = Geriatric Depression Scale; ADL = activities of daily living.

Interactions between genetic risk and physical activity

Table 2 indicates that significant 2 (Risk) × 2 (PA) interactions were observed for FA in 13 tracts: three long association (superior longitudinal fasciculus, bilateral sagittal stratum), four limbic association (bilateral cingulum, bilateral fornix/stria terminalis), and six projection (bilateral anterior limb of the internal capsule, bilateral anterior corona radiata, left posterior corona radiata, and left superior corona radiata). Inspection of the interaction revealed that within the Low Risk groups, FA was greater in the Low Risk-High PA compared to the Low Risk-Low PA group. However, the opposite pattern was observed in the High Risk groups: FA was lower in the High Risk-High PA compared to the High Risk-Low PA group. Fig. 2 displays mean FA values for each group in four (of 13) representative tracts in which there was a significant interaction between genetic risk and PA. The mean FA values for each group and the contrasts between groups for FA are shown in Supplemental Table 1.

Table 2. Interaction effects (2 Physical Activity (High, Low) × 2 APOE-ε4 Risk (High, Low) for diffusion tensor imaging measures within 25 white matter fiber tracts.

WM Tract	Fractional anisotropy (FA)		Mean diffusivity (MD)		Axial diffusivity (DA)		Radial diffusivity (DR)	
	FA int. p	FA int. η_p^2	MD int. p	MD int. η_p^2	DA int. p	DA int. η_p^2	DR int. p	DR int. η_p^2
Long assoc.								
SLF, left	<i>.0016</i>	<i>.113</i>	<i>.0013</i>	<i>.119</i>	ns	–	<i>.0005</i>	<i>.138</i>
SLF, right	<i>.0443</i>	<i>.048</i>	<i>.0020</i>	<i>.110</i>	<i>.0177</i>	<i>.066</i>	<i>.0025</i>	<i>.106</i>
SS, left	<i><.0001</i>	<i>.194</i>	<i>.0027</i>	<i>.104</i>	ns	–	<i>.0001</i>	<i>.167</i>
SS, right	<i>.0005</i>	<i>.138</i>	<i>.0036</i>	<i>.099</i>	ns	–	<i>.0003</i>	<i>.146</i>
UNC, left	ns	–	ns	–	ns	–	<i>.0499</i>	<i>.046</i>
UNC, right	<i>.0340</i>	<i>.053</i>	ns	–	ns	–	ns	–
Limbic assoc.								
CGC, left	<i>.0033</i>	<i>.099</i>	<i>.0130</i>	<i>.072</i>	ns	–	<i>.0006</i>	<i>.135</i>
CGC, right	<i>.0092</i>	<i>.079</i>	<i>.0096</i>	<i>.078</i>	ns	–	<i>.0026</i>	<i>.104</i>
CGH, left	<i>.0379</i>	<i>.051</i>	ns	–	ns	–	ns	–
CGH, right	<i>.0438</i>	<i>.048</i>	ns	–	ns	–	<i>.0255</i>	<i>.059</i>
FxS, left	<i>.0206</i>	<i>.063</i>	ns	–	ns	–	ns	–
FxS, right	<i>.0042</i>	<i>.095</i>	<i>.0411</i>	<i>.049</i>	ns	–	<i>.0026</i>	<i>.105</i>
Commissural								
BCC	ns	–	ns	–	ns	–	ns	–
GCC	<i>.0450</i>	<i>.048</i>	ns	–	ns	–	ns	–
SCC	ns	–	<i>.0404</i>	<i>.050</i>	ns	–	ns	–
Projection								
ALIC, left	<i><.0001</i>	<i>.198</i>	<i>.0138</i>	<i>.071</i>	ns	–	<i>.0013</i>	<i>.117</i>
ALIC, right	<i>.0002</i>	<i>.158</i>	<i>.0408</i>	<i>.051</i>	ns	–	<i>.0051</i>	<i>.093</i>
PLIC, left	ns	–	<i>.0375</i>	<i>.052</i>	ns	–	ns	–
PLIC, right	ns	–	ns	–	ns	–	ns	–
ACR, left	<i>.0001</i>	<i>.180</i>	<i>.0218</i>	<i>.063</i>	ns	–	<i>.0030</i>	<i>.103</i>
ACR, right	<i>.0001</i>	<i>.171</i>	<i>.0199</i>	<i>.064</i>	ns	–	<i>.0043</i>	<i>.095</i>
PCR, left	<i>.0070</i>	<i>.084</i>	<i>.0380</i>	<i>.052</i>	ns	–	<i>.0222</i>	<i>.063</i>
PCR, right	<i>.0410</i>	<i>.050</i>	<i>.0136</i>	<i>.073</i>	<i>.0479</i>	<i>.047</i>	<i>.0117</i>	<i>.076</i>
SCR, left	<i>.0245</i>	<i>.059</i>	<i>.0006</i>	<i>.135</i>	ns	–	<i>.0004</i>	<i>.142</i>
SCR, right	<i>.0370</i>	<i>.051</i>	<i>.0003</i>	<i>.148</i>	<i>.0167</i>	<i>.067</i>	<i>.0004</i>	<i>.143</i>

Note: Values in ***bold italics*** exceed the false discovery rate (FDR) threshold for significance; other values are $p < .05$ but did not meet the FDR threshold; ns = not significant; η_p^2 = partial eta-squared; ACR = anterior corona radiata; ALIC = anterior limb of internal capsule; BCC = body of corpus callosum; CGC = cingulum (cingulate gyrus); CGH = cingulum-hippocampal projection; FxS = fornix (cres)/Stria terminalis; GCC = genu of corpus callosum; PCR = posterior corona radiate; PLIC = posterior limb of internal capsule; SCC = splenium of corpus callosum; SCR = superior corona radiata; SLF = superior longitudinal fasciculus; SS = sagittal stratum (includes inferior longitudinal fasciculus and inferior fronto-occipital fasciculus); UNC = uncinata fasciculus.

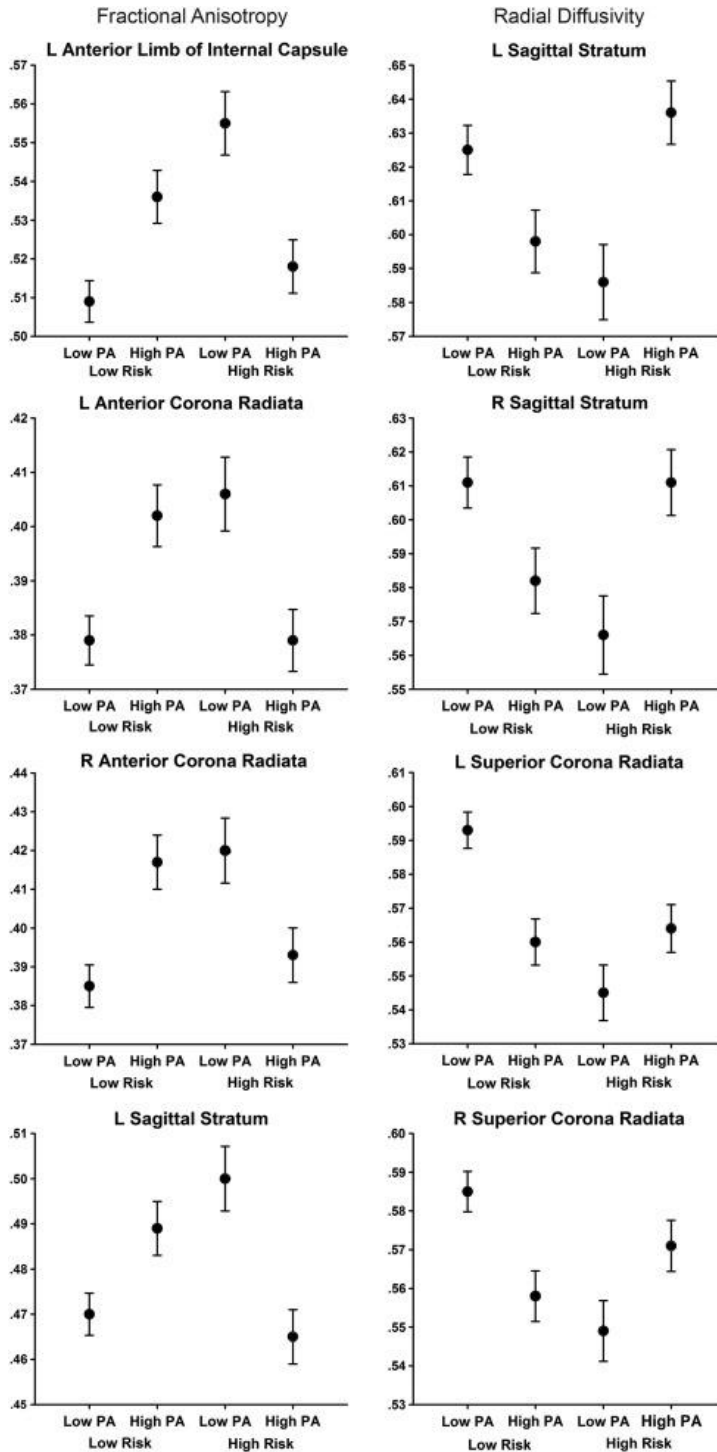


Fig. 2. (Left) Fractional anisotropy in the four groups of participants within the four WM tracts that had the largest Risk \times PA interaction effects. (Right) Radial diffusivity (mm^2/s) in the four groups of participants within the four WM tracts that had the largest Risk \times PA interaction effects. Error bars are the SEM.

Table 2 also presents significant 2 (Risk) \times 2 (PA) interactions for MD in 12 tracts: four long association (bilateral superior longitudinal fasciculus, bilateral sagittal stratum), two limbic association (bilateral cingulum) and six projection (left anterior limb of the internal capsule, bilateral anterior corona radiata, right posterior corona radiata, and bilateral superior corona radiata). Analysis of the interactions revealed that within the Low Risk groups, MD was lower in the Low Risk-High PA compared to the Low-Risk-Low PA group. However, the opposite pattern was observed in the High Risk groups; MD was greater in the High Risk-High PA compared to the High Risk-Low PA group. The mean MD values for each group and the contrasts between groups for MD are shown in Supplemental Table 2.

No significant 2 (Risk) \times 2 (PA) interactions were observed for DA. Three tracts (left superior longitudinal fasciculus, right posterior corona radiata, and right superior corona radiata) reached $p < .05$, but did not survive the FDR threshold to control for multiple comparisons (Table 2). The mean DA values for each group and the contrasts between groups for DA are shown in Supplemental Table 3.

Table 2 indicates that there were 16 tracts that demonstrated significant 2 (Risk) \times 2 (PA) interactions for DR: four long association (bilateral superior longitudinal fasciculus, bilateral sagittal stratum), four limbic association (bilateral cingulum-cingulate, right cingulum-hippocampal projection; right fornix/stria terminalis), and eight projection (bilateral anterior limb of the internal capsule, bilateral anterior corona radiata, bilateral posterior corona radiata, and bilateral superior corona radiata). Analysis of the interactions revealed that within the Low Risk groups, DR was lower in the Low Risk-High PA compared to the Low Risk-Low PA group. However, the opposite pattern was observed in the High Risk groups; DR was greater in the High Risk-High PA compared to the High Risk-Low PA group. The mean DR values for each group and the contrasts between groups for DR are shown in Supplemental Table 4.

The overall pattern of the interaction effects suggests that group differences in DR, coupled with the overall lack of group differences in DA, were driving the interaction effects for MD and FA (which are a function of the axial diffusivity eigenvector that defines DA and the two radial diffusivity eigenvectors that define DR). Fig. 2 displays the DR

values for each group in four (of 16) representative tracts in which there was a significant interaction between genetic risk and PA.

Main effects of genetic risk

No statistically significant main effects of genetic risk were observed on FA or DA in any of the 25 WM fiber tracts (Supplemental Tables 1 and 3, respectively). There were significant main effects of genetic risk on MD in six projection tracts (bilateral anterior limb of the internal capsule, left posterior limb of the internal capsule, bilateral posterior corona radiata, and left superior corona radiata; Supplemental Table 4). There were significant main effects of genetic risk on DR in four projection tracts (right anterior limb of the internal capsule, bilateral posterior corona radiata, and left superior corona radiata; Supplemental Table 4). For each significant main effect, the low risk groups had greater MD and DR values compared to the High Risk groups (see Supplemental Tables 2 and 4 for post-hoc comparisons).

Main effects of physical activity

One significant main effect of PA for FA was seen within the left fornix/stria terminalis, indicating greater FA on average in the Low PA groups. The only statistically significant post-hoc comparison indicated FA was greater in the High Risk-Low PA group compared to the High Risk-High PA group (Supplemental Table 1). There were no significant main effects of PA for MD (Supplemental Table 2), DA (Supplemental Table 3) or DR (Supplemental Table 4).

Associations between radial diffusivity and episodic memory performance

In order to shed light on the unexpected direction of the DR interactions between genetic risk and physical activity, we conducted a post-hoc analysis to determine if there were differences between the groups in the relationship between DR and cognitive function. Because the effect of PA on DR was in the opposite direction than hypothesized in the two high risk groups, we focused the analysis on the comparisons between the high and low PA groups within each of the

two risk groups. Pearson correlation coefficients were computed between DR and AVLT Trials 1–5, AVLT immediate recall, and AVLT delayed recall scores in each of the 25 WM tracts. The resulting magnitudes of the correlations between DR and the AVLT scores were directly compared (using Fisher's r to z transformation) between the High PA and Low PA groups within each APOE risk group, and the FDR threshold was applied to determine the statistical significance of each group comparison. We hypothesized that radial diffusivity would be negatively correlated with episodic memory performance in each group (greater DR associated with lower episodic memory performance), but that the magnitude of the negative correlations would be attenuated in the High Risk-Low PA group compared to their High PA counterparts.

As expected, the low risk groups demonstrated significant negative correlations between DR and AVLT performance and no significant differences were observed between High PA and Low PA groups in terms of the magnitude of the correlations between DR and AVLT scores. In the Low Risk-High PA group, there were significant negative correlations between DR and AVLT immediate recall in the left cingulum bundle ($r = -.38, p = .04$), left cingulum-hippocampal tract ($r = -.48, p = .03$), and body of the corpus callosum ($r = -.50, p = .02$); in the Low Risk-Low PA group, there were significant negative correlations between DR and AVLT delayed recall score in the left and right anterior limb of the internal capsule ($r = -.38, p = .04$; $r = -.37, p = .04$, respectively), the right superior corona radiata ($r = -.41, p = .02$), and the genu of the corpus callosum ($r = -.347, p = .05$). Similarly, in the High Risk-High PA group, there were significant negative correlations between DR and AVLT immediate recall performance in the left and right longitudinal fasciculus and left and right sagittal stratum ($r = -.48, p = .03$; $r = -.46, p = .04$, respectively), the posterior limb of the internal capsule ($r = -.53, p = .02$) and the splenium of the corpus callosum ($r = -.51, p = .02$).

In contrast, within the high risk groups there were eight WM tracts in which the correlations between DR and the AVLT delayed recall score were significantly different between the High PA and Low PA groups (bilateral ALIC, bilateral CGC, bilateral FxS, right SLF and right PLIC; all met FDR threshold, $p < .01$, one-tailed). As shown in Fig. 3, there were significant positive correlations between DR and AVLT delayed recall score in the High Risk-Low PA group compared to

the negative or near zero correlations in the High Risk-High PA group, and the group differences in the correlation coefficients were statistically significant (FDR-corrected for multiple comparisons). A similar pattern emerged when comparing correlations between DR and AVLT immediate recall score in the two High Risk groups (three comparisons, not shown, met the FDR threshold; bilateral CGC and right SLF, all $p < .005$, one-tailed).

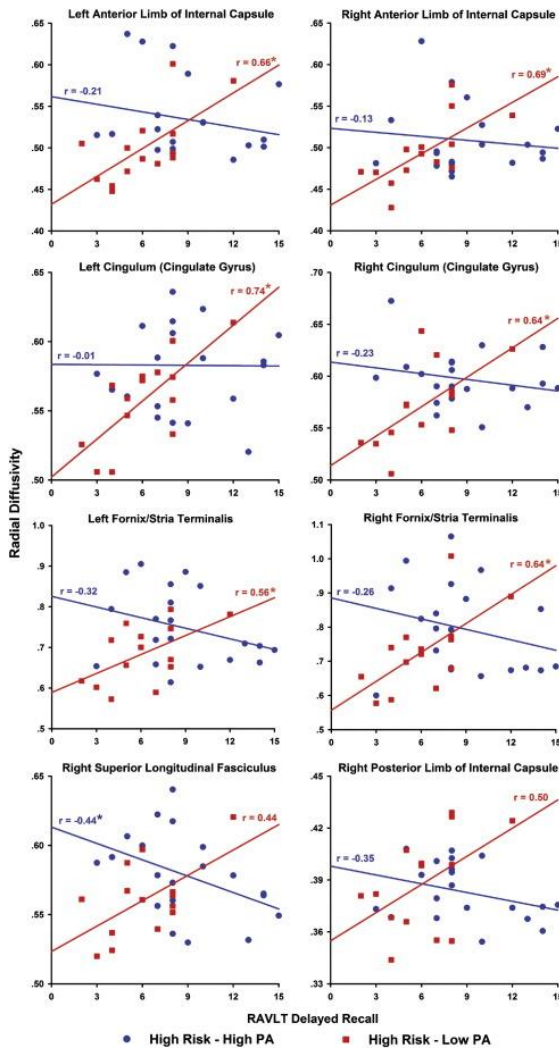


Fig. 3. Scatter plots and fitted linear regression lines showing the relationships between radial diffusivity and Rey Auditory Verbal Learning Test delayed recall performance in the High Risk-Low PA (red squares) and High Risk-High PA (blue circles) groups in eight white matter fiber tracts. In each fiber tract, the difference in the magnitude of the correlation was significantly different between the groups (FDR-corrected, $p < .05$). An asterisk indicates that the correlation was significant ($p < .05$) compared to 0.

Discussion

Interactions between genetic risk and physical activity participation

Based on previous studies that have reported stronger effects of PA on cognition, risk for cognitive decline, and hippocampal atrophy among *APOE-ε4* allele carriers, we hypothesized that the effects of PA on DTI metrics would be greater in the *APOE-ε4* allele carriers compared to non-carriers. While this hypothesis was supported, the results were not in the expected direction. Participants at greater genetic risk who reported engaging in greater amounts of PA had *lower* FA and *greater* diffusivity in several WM tracts compared to their physically inactive *APOE-ε4* allele carrying counterparts. The group differences in FA and MD, together with the lack of group differences in DA, indicate these effects are primarily driven by the group differences in DR (Acosta-Cabronero et al., 2010).

Increased radial diffusivity has been observed in AD patients (Bosch et al., 2012), and has been hypothesized to reflect axonal demyelination (Song et al., 2002). However, this proposed mechanism does not explain the greater radial diffusivity we observed in healthy physically active compared to physically inactive *ε4* carriers and it is not consistent with their cognitive trajectory. Our previous reports from a subsample of this cohort indicated that over the 18 months prior to the current study, the physically active *ε4* carriers were less likely to decline on tests of episodic memory function (Woodard et al., 2012) and displayed maintenance of hippocampal volume that was comparable to *ε4* non-carriers (Smith et al., 2014). Moreover, the physically active *ε4* carriers had greater semantic memory-related activation compared to the group of physically inactive *ε4* carriers (Smith et al., 2011), which we have shown to predict cognitive stability over 18 months (Woodard et al., 2010). This pattern of activation appears to reflect a successful neural compensatory response over 5 years (Rao et al., 2015). In contrast, the combination of being physically inactive and at increased genetic risk for AD, despite being cognitively intact with normal hippocampal volumes at baseline, resulted in greater probability of cognitive decline and hippocampal atrophy over 18 months (Smith et al.,

2014 and Woodard et al., 2012). These interactive effects between PA and APOE genotype have also been reported for brain amyloid accumulation in healthy older adults, as measured by PET and CSF biomarkers, with only the physically inactive $\epsilon 4$ carriers showing a substantial amyloid burden (Head et al., 2012). The common thread among these studies is that PA appears to moderate the effect of the *APOE- $\epsilon 4$* allele and results in normalization of the biomarker for AD progression, with the physically active $\epsilon 4$ carriers more closely resembling those at low genetic risk in both their cognitive trajectory and brain structural profile. However, being a physically inactive *APOE- $\epsilon 4$* allele carrier appears to substantially increase the likelihood for cognitive decline and neurodegeneration.

The overall pattern of our results indicates that the radial diffusivity in the High Risk-High PA group was more similar to the Low Risk groups. Clues to the meaning of these results lie within the High Risk-Low PA group, who showed unexpectedly low radial diffusivity compared to the other groups. One possible explanation is that there were fewer crossing fibers within these WM tracts in the High Risk-Low PA group. Crossing fibers are known to be more prominent in projection fiber tracts such as the superior corona radiata and the presence of more crossing fibers leads to greater values for radial diffusivity using scalar diffusion-weighted imaging metrics (Pierpaoli et al., 2001). The loss of crossing fibers in these WM tracts due to a neurodegenerative process may result in a reduction in radial diffusivity and increased FA, possibly resulting in lesser structural and functional connectivity within the affected neural networks (Pierpaoli et al., 2001). This selective neurodegenerative effect, leading to greater FA, has been demonstrated in AD and MCI patients compared to healthy controls within the centrum semiovale (which is continuous with the superior corona radiata) where there are more crossing fibers, but not the corpus callosum, where white matter fiber direction is more uniform (Douaud et al., 2011). Our observed interaction effects were restricted to long association, limbic association, and projection fiber tracts, where crossing fibers are more likely to be present. Two of the largest interaction effects for DR were observed in the superior corona radiata (see Table 2 and Fig. 2), consistent with the results reported by Douaud and colleagues. Importantly, there were no significant differences between the groups within the commissural fiber tracts or for axial diffusivity in any of the WM tracts. These effects are

consistent with selective degenerative processes that preserve the tract along its primary longitudinal axis (Douaud et al., 2011). The relationships we observed between radial diffusivity and episodic memory performance support this interpretation.

In the low risk participants, and among the physically active $\epsilon 4$ carriers, greater radial diffusivity was associated with lower word list learning performance, as might be expected. However, in the High Risk-Low PA group, this association was reversed, and greater radial diffusivity was associated with *greater* delayed and immediate recall performance on the AVLT. Thus, it is plausible that the significantly lower cognitive performance in the High Risk-Low PA group is related to the loss or thinning of crossing WM fibers within WM tracts that serve cortical and hippocampal regions involved in episodic memory encoding and retrieval. These findings require replication using animal models and human studies with higher resolution DTI sequences that would more accurately determine WM crossing fiber differences between physically active and physically inactive $\epsilon 4$ carriers.

Main effects for genetic risk

We found very little evidence for overall differences in WM diffusivity between *APOE- $\epsilon 4$* carriers and non-carriers (see Supplemental Tables). In the current study, the main effects for genetic risk were small and limited to a few fiber tracts for MD and DR. However, these effects were in the opposite direction as would be predicted due to the interactions with PA in the high-risk groups and many did not survive correction for multiple comparisons. Several previous studies have compared DTI measures between older adults at low versus high genetic risk for AD and found mixed findings. Some studies report lower FA and/or greater diffusivity among *APOE- $\epsilon 4$* carriers versus non-carriers (Dowell et al., 2013, Gold et al., 2010, Heise et al., 2011, Nierenberg et al., 2005, Persson et al., 2006 and Smith et al., 2010), while others report no differences between these groups (Bendlin et al., 2010, Honea et al., 2009, Matura et al., 2014, Nyberg and Salami, 2014, O'Dwyer et al., 2012 and Patel et al., 2013). It is possible that these mixed reports, and the relatively limited effects that have been reported, are because

the moderating influence of PA and its potential interactive effects with APOE genotype have not been considered.

Main effects for physical activity

Previous studies in healthy older adults have reported that greater cardiorespiratory fitness was associated with higher FA in the cingulum bundle (Marks et al., 2011, Marks et al., 2007 and Tian et al., 2014b), uncinate fasciculus (Marks et al., 2007), and corpus callosum (Johnson et al., 2012), and lower mean and radial diffusivity in the entorhinal cortex (Tian et al., 2014b) and corpus callosum (Johnson et al., 2012), respectively. One exercise training study found that increased cardiorespiratory fitness in the walking intervention group, but not in the stretching control group, was associated with greater FA in the frontal WM tracts (Voss et al., 2012). In another study, master athletes (mean age 72 years with more than 15 years of endurance training) had higher FA values compared to sedentary older adults in the right superior corona radiata, bilateral superior longitudinal fasciculus, right inferior fronto-occipital fasciculus, and left inferior longitudinal fasciculus, and lower MD values in the left posterior thalamic radiation and left cingulum hippocampus tract (Tseng et al., 2013). Self-reported PA in healthy older adults has been associated with lower MD in the medial temporal lobe and cingulate cortex (Tian et al., 2014a).

In all of these previously published studies, the influence of the *APOE-ε4* allele was not reported. When the presence or absence of the *APOE-ε4* allele was taken into consideration in the current study, the large interaction effects between genetic risk and PA superseded the main effects of PA. However, comparison between only the two low risk groups reveals that the effects of PA were consistent with the prior literature. The Low Risk-High PA group, compared to the Low Risk-Low PA group, had significantly greater FA in the left sagittal stratum, bilateral anterior limb of the internal capsule, and along nearly the entire corona radiata (Supplemental Table 1). For WM diffusivity, the Low Risk-High PA participants had lower DR in the bilateral superior longitudinal fasciculus, sagittal stratum, cingulum, anterior limb of the internal capsule, and the posterior and superior corona radiata (Supplemental Table 4), which were mirrored in the effects on MD

(Supplemental Table 2). In contrast, the directions of the main effects of PA were reversed in the higher risk groups. Finally, in this study and in previous studies, few if any effects of PA or fitness have been found for axial diffusivity.

Potential mechanisms

There are several potential neurophysiological mechanisms for exercise and PA to protect brain structure and function in old age. PA is well known for its neurotrophic effects in rodents that support neurogenesis in the dentate gyrus (Trejo et al., 2001 and van Praag et al., 2005), effects likely to occur in humans as well (Erickson et al., 2011 and Pereira et al., 2007). Exercise has been shown to improve cholinergic function and to oppose the actions of acetylcholinesterase in the hippocampus and cerebral cortex of rats (Ben et al., 2009). In addition, cholinergic enhancement due to PA may increase cerebral blood flow, enhance neural activation, and possibly reduce amyloid burden (Adlard et al., 2005 and Head et al., 2012). The neuroprotective mechanisms of PA specific to WM integrity in $\epsilon 4$ -carriers are less well understood. Rodent studies suggest PA counteracts the physiologic impact of the *APOE- $\epsilon 4$ allele*, and the resultant reduction in availability of apolipoprotein-E, through improved brain lipid metabolism, reduced neuroinflammation, and/or augmented cholinergic function (Intlekofer and Cotman, 2013). Exercise in $\epsilon 4$ mice leads to normalization of tyrosine kinase B receptors, which have a high affinity for BDNF (Nichol et al., 2009) and to increased anti-inflammatory cytokines (Fukao et al., 2010). The selective sparing of WM tracts in the current study may also be related to exercise-induced spinogenesis and/or dendritic branching along axons (Eadie et al., 2005), which is compromised by the *APOE- $\epsilon 4$ allele* in mouse models of AD (Dumanis et al., 2009).

Limitations

This study is limited by its cross sectional design. A causal pathway between PA and WM diffusivity cannot be determined until a randomized controlled trial is conducted to compare the effects of exercise training on changes in white matter diffusivity between *APOE- $\epsilon 4$ allele* carriers and non-carriers. Unfortunately, we were not able to

obtain DTI data at the baseline session 18 months before the current data were collected. It will be important for future studies to track the longitudinal changes in WM integrity as a function of both genetic risk and PA behavior, to consider the independent role of family history for AD, and to determine if these effects extend beyond our predominantly Caucasian sample. As noted in our previous work, this study is also limited by the use of self-reported leisure time PA, rather than an objective measurement of cardiorespiratory fitness, such as the maximal rate of oxygen consumption (VO_{2max}). The SBAS, however, has been shown in large samples to be associated with estimated caloric expenditure during PA and to be dose-dependently related to cardiovascular risk biomarkers (Taylor-Piliae et al., 2006).

Conclusions

Consistent with previous studies in healthy older adults, greater levels of PA were associated with greater FA and lower radial diffusivity within association and projection WM tracts in healthy older adults who did not possess the *APOE-ε4* allele. However, these effects of PA were reversed in older adults who were at increased genetic risk for AD and who had exhibited episodic memory decline over the past 18 months. In less physically active and genetically at risk individuals, radial diffusivity was lower compared to those with greater levels of leisure time physical activity who also possessed the *APOE-ε4* allele. Moreover, in several tracts that serve learning and memory processes, lower radial diffusivity was significantly correlated with lower episodic memory performance in the physically inactive at-risk group. While it is possible that PA may protect myelin and thus reduce radial diffusion, our findings call into question the common interpretation that greater radial diffusivity inevitably reflects demyelination and neurodegeneration. We hypothesize that PA may specifically protect *APOE-ε4* allele carriers against the selective loss of white matter fibers in projection and association WM tracts, and furthermore, that physical inactivity may exacerbate the *APOE-ε4* related processes associated with degeneration of individual populations of white matter fibers in locations of crossing fibers. This hypothesis should be confirmed using more advanced diffusion-weighted imaging methods and randomized controlled exercise trials in humans. In addition, animal models should

be used to explore the mechanisms for these potential neuroprotective effects of physical activity in *APOE-ε4* allele carriers.

Conflicts of interest: The authors report no conflicts of interest.

Acknowledgments: This project was supported by NIH grant R01-AG022304. The content is solely the responsibility of the authors and does not necessarily represent the official views of the National Institute on Aging or the National Institutes of Health.

References

- Acosta-Cabronero et al., 2010. J. Acosta-Cabronero, G.B. Williams, G. Pengas, P.J. Nestor. Absolute diffusivities define the landscape of white matter degeneration in Alzheimer's disease. *Brain*, 133 (Pt 2) (2010), pp. 529–539
- Adlard et al., 2005. P.A. Adlard, V.M. Perreau, V. Pop, C.W. Cotman. Voluntary exercise decreases amyloid load in a transgenic model of Alzheimer's disease. *J. Neurosci.*, 25 (17) (2005), pp. 4217–4221
- Barnes and Yaffe, 2011. D.E. Barnes, K. Yaffe. The projected effect of risk factor reduction on Alzheimer's disease prevalence. *Lancet Neurol.*, 10 (2011), pp. 819–828
- Bateman et al., 2012. R.J. Bateman, C. Xiong, T.L. Benzinger, A.M. Fagan, A. Goate, N.C. Fox, D.S. Marcus, N.J. Cairns, X. Xie, T.M. Blazey, D.M. Holtzman, A. Santacruz, V. Buckles, A. Oliver, K. Moulder, P.S. Aisen, B. Ghetti, W.E. Klunk, E. McDade, R.N. Martins, C.L. Masters, R. Mayeux, J.M. Ringman, M.N. Rossor, P.R. Schofield, R.A. Sperling, S. Salloway, J.C. Morris. Clinical and biomarker changes in dominantly inherited Alzheimer's disease. *N. Engl. J. Med.*, 367 (9) (2012), pp. 795–804
- Beckett et al., 2015. M.W. Beckett, C.I. Arden, M.A. Rotondi. A meta-analysis of prospective studies on the role of physical activity and the prevention of Alzheimer's disease in older adults. *BMC Geriatr.*, 15 (1) (2015), p. 9
- Behrens et al., 2003. M.W. Behrens, M. Woolrich, H. Jenkinson, R.G. Johansen-Berg, S. Nunes, P.M. Clare. Characterization and propagation of uncertainty in diffusion-weighted MR imaging. *Magn. Reson. Med.*, 50 (2003), pp. 1077–1088
- Ben et al., 2009. J. Ben, F.M. Soares, F. Cechetti, F.C. Vuaden, C.D. Bonan, C.A. Netto, A.T. Wyse. Exercise effects on activities of Na(+), K(+)-ATPase, acetylcholinesterase and adenine nucleotides hydrolysis in ovariectomized rats. *Brain Res.*, 1302 (2009), pp. 248–255

- Bendlin et al., 2010. B.B. Bendlin, M.L. Ries, E. Canu, A. Sodhi, M. Lazar, A.L. Alexander, C.M. Carlsson, M.A. Sager, S. Asthana, S.C. Johnson. White matter is altered with parental family history of Alzheimer's disease. *Alzheimers Dement.*, 6 (5) (2010), pp. 394–403
- Bird, 2008. T.D. Bird. Genetic aspects of Alzheimer disease. *Genet. Med.*, 10 (4) (2008), pp. 231–239
- Bosch et al., 2012. B. Bosch, E.M. Arenaza-Urquijo, L. Rami, R. Sala-Llonch, C. Junque, C. Sole-Padullés, C. Pena-Gomez, N. Bargallo, J.L. Molinuevo, D. Bartres-Faz. Multiple DTI index analysis in normal aging, amnesic MCI and AD. Relationship with neuropsychological performance. *Neurobiol. Aging*, 33 (1) (2012), pp. 61–74
- Clark et al., 2008 C.M. Clark, C. Davatzikos, A. Borthakur, A. Newberg, S. Leight, V.M. Lee, J.Q. Trojanowski. Biomarkers for early detection of Alzheimer pathology. *Neurosignals*, 16 (1) (2008), pp. 11–18
- Colcombe et al., 2004. S.J. Colcombe, A.F. Kramer, K.I. Erickson, P. Scalf, E. McAuley, N.J. Cohen, A. Webb, G.J. Jerome, D.X. Marquez, S. Elavsky. Cardiovascular fitness, cortical plasticity, and aging. *Proc. Natl. Acad. Sci. U. S. A.*, 101 (9) (2004), pp. 3316–3321
- Cox, 1996. R. Cox. AFNI: software for analysis and visualization of functional magnetic resonance images. *Comput. Biomed. Res.*, 29 (1996), pp. 162–173
- Douaud et al., 2011. G. Douaud, S. Jbabdi, T.E. Behrens, R.A. Menke, A. Gass, A.U. Monsch, A. Rao, B. Whitcher, G. Kindlmann, P.M. Matthews, S. Smith. DTI measures in crossing-fibre areas: increased diffusion anisotropy reveals early white matter alteration in MCI and mild Alzheimer's disease. *NeuroImage*, 55 (3) (2011), pp. 880–890
- Dowell et al., 2013. N.G. Dowell, T. Ruest, S.L. Evans, S.L. King, N. Tabet, P.S. Tofts, J.M. Rusted. MRI of carriers of the apolipoprotein E e4 allele-evidence for structural differences in normal-appearing brain tissue in e4 + relative to e4 – young adults. *NMR Biomed.*, 26 (6) (2013), pp. 674–682
- Dumanis et al., 2009. S.B. Dumanis, J.A. Tesoriero, L.W. Babus, M.T. Nguyen, J.H. Trotter, M.J. Ladu, E.J. Weeber, R.S. Turner, B. Xu, G.W. Rebeck, H.S. Hoe. ApoE4 decreases spine density and dendritic complexity in cortical neurons in vivo. *J. Neurosci.*, 29 (48) (2009), pp. 15317–15322
- Eadie et al., 2005. B.D. Eadie, V.A. Redila, B.R. Christie. Voluntary exercise alters the cytoarchitecture of the adult dentate gyrus by increasing cellular proliferation, dendritic complexity, and spine density. *J. Comp. Neurol.*, 486 (1) (2005), pp. 39–47
- Erickson et al., 2011. K.I. Erickson, M.W. Voss, R.S. Prakash, C. Basak, A. Szabo, L. Chaddock, J.S. Kim, S. Heo, H. Alves, S.M. White, T.R. Wojcicki, E. Mailey, V.J. Vieira, S.A. Martin, B.D. Pence, J.A. Woods, E.

- McAuley, A.F. Kramer. Exercise training increases size of hippocampus and improves memory. *Proc. Natl. Acad. Sci. U. S. A.*, 108 (7) (2011), pp. 3017–3022
- Etgen et al., 2010. T. Etgen, D. Sander, U. Huntgeburth, H. Poppert, H. Forstl, H. Bickel. Physical activity and incident cognitive impairment in elderly persons: the INVADE study. *Arch. Intern. Med.*, 170 (2) (2010), pp. 186–193
- Folstein et al., 1975. M.F. Folstein, S.E. Folstein, P.R. McHugh. "Mini-Mental State": a practical method for grading the cognitive state of patients for the clinician. *J. Psychiatry Res.*, 12 (1975), pp. 189–198
- Fukao et al., 2010. K. Fukao, K. Shimada, H. Naito, K. Sumiyoshi, N. Inoue, T. Iesaki, A. Kume, T. Kiyanagi, M. Hiki, K. Hirose, R. Matsumori, H. Ohsaka, Y. Takahashi, S. Toyoda, S. Itoh, T. Miyazaki, N. Tada, H. Daida. Voluntary exercise ameliorates the progression of atherosclerotic lesion formation via anti-inflammatory effects in apolipoprotein E-deficient mice. *J. Atheroscler. Thromb.*, 17 (12) (2010), pp. 1226–1236
- Gold et al., 2010. B.T. Gold, D.K. Powell, A.H. Andersen, C.D. Smith. Alterations in multiple measures of white matter integrity in normal women at high risk for Alzheimer's disease. *NeuroImage*, 52 (4) (2010), pp. 1487–1494
- Head et al., 2012. D. Head, J.M. Bugg, A.M. Goate, A.M. Fagan, M.A. Mintun, T. Benzinger, D.M. Holtzman, J.C. Morris. Exercise engagement as a moderator of the effects of APOE genotype on amyloid deposition. *Arch. Neurol.*, 69 (5) (2012), pp. 636–643
- Heise et al., 2011. V. Heise, N. Filippini, K.P. Ebmeier, C.E. Mackay. The APOE varepsilon4 allele modulates brain white matter integrity in healthy adults. *Mol. Psychiatry*, 16 (9) (2011), pp. 908–916
- Honea et al., 2009. R.A. Honea, E. Vidoni, A. Harsha, J.M. Burns. Impact of APOE on the healthy aging brain: a voxel-based MRI and DTI study. *J. Alzheimers Dis.*, 18 (3) (2009), pp. 553–564
- Intlekofer and Cotman, 2013. K.A. Intlekofer, C.W. Cotman. Exercise counteracts declining hippocampal function in aging and Alzheimer's disease. *Neurobiol. Dis.*, 57 (2013), pp. 47–55
- Johnson et al., 2012. N.F. Johnson, C. Kim, J.L. Clasey, A. Bailey, B.T. Gold. Cardiorespiratory fitness is positively correlated with cerebral white matter integrity in healthy seniors. *NeuroImage*, 59 (2) (2012), pp. 1514–1523
- Jurica et al., 2001. P.J. Jurica, C.L. Leittten, S. Mattis. *Dementia Rating Scale-2 Professional Manual*. Psychological Assessment Resources, Lutz, FL (2001)

- Lane and Farlow, 2005. R.M. Lane, M.R. Farlow. Lipid homeostasis and apolipoprotein E in the development and progression of Alzheimer's disease. *J. Lipid Res.*, 46 (5) (2005), pp. 949–968
- Lawton and Brody, 1969. M.P. Lawton, E.M. Brody. Assessment of older people: self-maintaining and instrumental activities of daily living. *Gerontologist*, 9 (3) (1969), pp. 179–186
- Marks et al., 2007. B.L. Marks, D.J. Madden, B. Bucur, J.M. Provenzale, L.E. White, R. Cabeza, S.A. Huettel. Role of aerobic fitness and aging on cerebral white matter integrity. *Ann. N. Y. Acad. Sci.*, 1097 (2007), pp. 171–174
- Marks et al., 2011. B.L. Marks, L.M. Katz, M. Styner, J.K. Smith. Aerobic fitness and obesity: relationship to cerebral white matter integrity in the brain of active and sedentary older adults. *Br. J. Sports Med.*, 45 (15) (2011), pp. 1208–1215
- Matura et al., 2014. S. Matura, D. Prvulovic, A. Jurcoane, D. Hartmann, J. Miller, M. Scheibe, L. O'Dwyer, V. Oertel-Knochel, C. Knochel, B. Reinke, T. Karakaya, F. Fusser, J. Pantel. Differential effects of the ApoE4 genotype on brain structure and function. *NeuroImage*, 89 (2014), pp. 81–91
- Mori et al., 2008. S. Mori, K. Oishi, H. Jiang, L. Jiang, X. Li, K. Akhter, K. Hua, A.V. Faria, A. Mahmood, R. Woods, A.W. Toga, G.B. Pike, P.R. Neto, A. Evans, J. Zhang, H. Huang, M.I. Miller, P. van Zijl, J. Mazziotta. Stereotaxic white matter atlas based on diffusion tensor imaging in an ICBM template. *NeuroImage*, 40 (2) (2008), pp. 570–582
- Nichol et al., 2009. K. Nichol, S.P. Deeny, J. Seif, K. Camaclang, C.W. Cotman. Exercise improves cognition and hippocampal plasticity in APOE epsilon4 mice. *Alzheimers Dement.*, 5 (4) (2009), pp. 287–294
- Nierenberg et al., 2005. J. Nierenberg, N. Pomara, M.J. Hoptman, J.J. Sidtis, B.A. Ardekani, K.O. Lim. Abnormal white matter integrity in healthy apolipoprotein E epsilon4 carriers. *Neuroreport*, 16 (12) (2005), pp. 1369–1372
- Nyberg and Salami, 2014. L. Nyberg, A. Salami. The APOE epsilon4 allele in relation to brain white-matter microstructure in adulthood and aging. *Scand. J. Psychol.*, 55 (3) (2014), pp. 263–267
- O'Dwyer et al., 2012. L. O'Dwyer, F. Lambertson, S. Matura, M. Scheibe, J. Miller, D. Rujescu, D. Prvulovic, H. Hampel. White matter differences between healthy young ApoE4 carriers and non-carriers identified with tractography and support vector machines. *PLoS One*, 7 (4) (2012), p. e36024
- Patel et al., 2013. K.T. Patel, M.C. Stevens, G.D. Pearlson, A.M. Winkler, K.A. Hawkins, P. Skudlarski, L.O. Bauer. Default mode network activity and white matter integrity in healthy middle-aged ApoE4 carriers. *Brain Imaging Behav.*, 7 (1) (2013), pp. 60–67

- Pereira et al., 2007. A.C. Pereira, D.E. Huddleston, A.M. Brickman, A.A. Sosunov, R. Hen, G.M. McKhann, R. Sloan, F.H. Gage, T.R. Brown, S.A. Small. An in vivo correlate of exercise-induced neurogenesis in the adult dentate gyrus. *Proc. Natl. Acad. Sci. U. S. A.*, 104 (13) (2007), pp. 5638–5643
- Persson et al., 2006. J. Persson, J. Lind, A. Larsson, M. Ingvar, M. Cruts, C. Van Broeckhoven, R. Adolfsson, L.G. Nilsson, L. Nyberg. Altered brain white matter integrity in healthy carriers of the APOE epsilon4 allele: a risk for AD? *Neurology*, 66 (7) (2006), pp. 1029–1033
- Pierpaoli et al., 2001. C. Pierpaoli, A. Barnett, S. Pajevic, R. Chen, L.R. Penix, A. Virta, P. Basser. Water diffusion changes in Wallerian degeneration and their dependence on white matter architecture. *NeuroImage*, 13 (6 Pt 1) (2001), pp. 1174–1185
- Poirier, 2000. J. Poirier. Apolipoprotein E and Alzheimer's disease. A role in amyloid catabolism. *Ann. N. Y. Acad. Sci.*, 924 (2000), pp. 81–90
- Rao et al., 2015. S.M. Rao, A. Bonner-Jackson, K.A. Nielson, M. Seidenberg, J.C. Smith, J.L. Woodard, S. Durgerian. Genetic risk for Alzheimer's disease alters the five-year trajectory of semantic memory activation in cognitively intact elders. *NeuroImage*, 111C (2015), pp. 136–146
- Reiman et al., 2010. E.M. Reiman, J.B. Langbaum, P.N. Tariot. Alzheimer's prevention initiative: a proposal to evaluate presymptomatic treatments as quickly as possible. *Biomark. Med.*, 4 (1) (2010), pp. 3–14
- Rey, 1958. A. Rey. *L'examen clinique en psychologie*. Presses Universitaires de France, Paris (1958)
- Sager et al., 2005. M.A. Sager, B. Hermann, A. La Rue. Middle-aged children of persons with Alzheimer's disease: APOE genotypes and cognitive function in the Wisconsin Registry for Alzheimer's Prevention. *J. Geriatr. Psychiatry Neurol.*, 18 (4) (2005), pp. 245–249
- Saunders et al., 1996. A.M. Saunders, O. Hulette, K.A. Welsh-Bohmer, D.E. Schmechel, B. Crain, J.R. Burke, M.J. Alberts, W.J. Strittmatter, J.C. Breitner, C. Rosenberg. Specificity, sensitivity, and predictive value of apolipoprotein-E genotyping for sporadic Alzheimer's disease. *Lancet*, 348 (9020) (1996), pp. 90–93
- Schuit et al., 2001. A.J. Schuit, E.J. Feskens, L.J. Launer, D. Kromhout. Physical activity and cognitive decline, the role of the apolipoprotein e4 allele. *Med. Sci. Sports Exerc.*, 33 (5) (2001), pp. 772–777
- Smith, 2002. S.M. Smith. Fast robust automated brain extraction. *Hum. Brain Mapp.*, 17 (2002), pp. 143–155
- Smith et al., 2006. S.M. Smith, M. Jenkinson, H. Johansen-Berg, D. Ruckert, T.E. Nichols, C.E. Mackay. Tract-based spatial statistics: voxelwise analysis of multi-subject diffusion data. *NeuroImage*, 31 (2006), pp. 1487–1505

- Smith et al., 2010. C.D. Smith, H. Chebrolu, A.H. Andersen, D.A. Powell, M.A. Lovell, S. Xiong, B.T. Gold. White matter diffusion alterations in normal women at risk of Alzheimer's disease. *Neurobiol. Aging*, 31 (7) (2010), pp. 1122–1131
- Smith et al., 2011. J.C. Smith, K.A. Nielson, J.L. Woodard, M. Seidenberg, S. Durgerian, P. Antuono, A.M. Butts, N.C. Hantke, M.A. Lancaster, S.M. Rao. Interactive effects of physical activity and APOE-epsilon4 on BOLD semantic memory activation in healthy elders. *NeuroImage*, 54 (1) (2011), pp. 635–644
- Smith et al., 2013. J.C. Smith, K.A. Nielson, P. Antuono, J.-A. Lyons, R.J. Hanson, A.M. Butts, N.C. Hantke, M.D. Verber. Semantic memory functional MRI and cognitive function after exercise intervention in mild cognitive impairment. *J. Alzheimers Dis.*, 37 (1) (2013), pp. 197–215
- Smith et al., 2014. J.C. Smith, K.A. Nielson, J.L. Woodard, M. Seidenberg, S. Durgerian, K.E. Hazlett, C.M. Figueroa, C.C. Kandah, C.D. Kay, M.A. Matthews, S.M. Rao. Physical activity reduces hippocampal atrophy in elders at genetic risk for Alzheimer's disease. *Front. Aging Neurosci.*, 6 (61) (2014), pp. 1–7
- Song et al., 2002. S.K. Song, S.W. Sun, M.J. Ramsbottom, C. Chang, J. Russell, A.H. Cross. Dysmyelination revealed through MRI as increased radial (but unchanged axial) diffusion of water. *NeuroImage*, 17 (3) (2002), pp. 1429–1436
- Sperling et al., 2014. R. Sperling, E. Mormino, K. Johnson. The evolution of preclinical Alzheimer's disease: implications for prevention trials. *Neuron*, 84 (3) (2014), pp. 608–622
- Taylor-Piliae et al., 2006. R.E. Taylor-Piliae, L.C. Norton, W.L. Haskell, M.H. Mahbouda, J.M. Fair, C. Iribarren, M.A. Hlatky, A.S. Go, S.P. Fortmann. Validation of a new brief physical activity survey among men and women aged 60-69 years. *Am. J. Epidemiol.*, 164 (6) (2006), pp. 598–606
- Taylor-Piliae et al., 2007. R.E. Taylor-Piliae, W.L. Haskell, C. Iribarren, L.C. Norton, M.H. Mahbouda, J.M. Fair, M.A. Hlatky, A.S. Go, S.P. Fortmann. Clinical utility of the Stanford brief activity survey in men and women with early-onset coronary artery disease. *J. Cardiopulm. Rehabil. Prev.*, 27 (4) (2007), pp. 227–232
- Taylor-Piliae et al., 2010. R.E. Taylor-Piliae, J.M. Fair, W.L. Haskell, A.N. Varady, C. Iribarren, M.A. Hlatky, A.S. Go, S.P. Fortmann. Validation of the Stanford Brief Activity Survey: examining psychological factors and physical activity levels in older adults. *J. Phys. Act. Health*, 7 (1) (2010), pp. 87–94
- Tian et al., 2014a. Q. Tian, K.I. Erickson, E.M. Simonsick, H.J. Aizenstein, N.W. Glynn, R.M. Boudreau, A.B. Newman, S.B. Kritchevsky, K. Yaffe,

- T.B. Harris, C. Rosano. Physical activity predicts microstructural integrity in memory-related networks in very old adults. *J. Gerontol. A Biol. Sci. Med. Sci.*, 69 (10) (2014), pp. 1284–1290
- Tian et al., 2014b. Q. Tian, E.M. Simonsick, K.I. Erickson, H.J. Aizenstein, N.W. Glynn, R.M. Boudreau, A.B. Newman, S.B. Kritchevsky, K. Yaffe, T. Harris, C. Rosano, Health, A.B.C.s. Cardiorespiratory fitness and brain diffusion tensor imaging in adults over 80 years of age. *Brain Res.*, 1588 (2014), pp. 63–72
- Trejo et al., 2001. J.L. Trejo, E. Carro, I. Torres-Aleman. Circulating insulin-like growth factor I mediates exercise-induced increases in the number of new neurons in the adult hippocampus. *J. Neurosci.*, 21 (5) (2001), pp. 1628–1634
- Tseng et al., 2013. B.Y. Tseng, T. Gundapuneedi, M.A. Khan, R. Diaz-Arrastia, B.D. Levine, H. Lu, H. Huang, R. Zhang. White matter integrity in physically fit older adults. *NeuroImage*, 82 (2013), pp. 510–516
- van Praag et al., 2005. H. van Praag, T. Shubert, C. Zhao, F.H. Gage. Exercise enhances learning and hippocampal neurogenesis in aged mice. *J. Neurosci.*, 25 (38) (2005), pp. 8680–8685
- Voss et al., 2012. M.W. Voss, S. Heo, R.S. Prakash, K.I. Erickson, H. Alves, L. Chaddock, A.N. Szabo, E.L. Mailey, T.R. Wojcicki, S.M. White, N. Gothe, E. McAuley, B.P. Sutton, A.F. Kramer. The influence of aerobic fitness on cerebral white matter integrity and cognitive function in older adults: Results of a one-year exercise intervention. *Hum. Brain Mapp.*, 34 (11) (2012), pp. 2972–2985
- Woodard et al., 2009. J.L. Woodard, M. Seidenberg, K.A. Nielson, P. Antuono, L. Guidotti, S. Durgerian, Q. Zhang, M. Lancaster, N. Hantke, A. Butts, S.M. Rao. Semantic memory activation in amnesic mild cognitive impairment. *Brain*, 132 (Pt 8) (2009), pp. 2068–2078
- Woodard et al., 2010. J.L. Woodard, M. Seidenberg, K.A. Nielson, J.C. Smith, P. Antuono, S. Durgerian, L. Guidotti, Q. Zhang, A. Butts, N. Hantke, M. Lancaster, S.M. Rao. Prediction of cognitive decline in healthy older adults using fMRI. *J. Alzheimers Dis.*, 21 (2010), pp. 871–885
- Woodard et al., 2012. J.L. Woodard, M.A. Sugarman, K.A. Nielson, J.C. Smith, M. Seidenberg, S. Durgerian, A. Butts, N. Hantke, M. Lancaster, M.A. Matthews, S.M. Rao. Lifestyle and genetic contributions to cognitive decline and hippocampal structure and function in healthy aging. *Curr. Alzheimer Res.*, 9 (4) (2012), pp. 436–446
- Yesavage, 1988. J.A. Yesavage. Geriatric Depression Scale. *Psychopharmacol. Bull.*, 24 (4) (1988), pp. 709–711

Appendix A. Supplementary data



Supplementary tables showing the mean and standard deviation values and statistical test results for FA, MD, DA, and DR in the four participant groups.

Supplemental Table 1. Mean and standard deviation (SD) values for fractional anisotropy (FA) in the four groups of participants within the 25 white matter (WM) fiber tracts.

WM Tract	Low Risk - High PA		Low Risk - Low PA		High Risk - High PA		High Risk - Low PA		Risk	PA	Risk * PA	LR-HPA vs. LR-LPA	LR-HPA vs. HR-HPA	LR-HPA vs. HR-LPA	LR-LPA vs. HR-HPA	LR-LPA vs. HR-LPA	HR-HPA vs. HR-LPA
	Mean	SD	Mean	SD	Mean	SD	Mean	SD	p-value	p-value	p-value						
Long Association																	
SLF_L	0.442	0.029	0.432	0.027	0.437	0.021	0.457	0.021	.174	.493	.0016	.044				.002	.012
SLF_R	0.434	0.029	0.427	0.028	0.433	0.015	0.441	0.020	.359	.854	.0443					.039	
SS_L	0.483	0.026	0.472	0.031	0.468	0.032	0.501	0.028	.602	.158	.00002	.017		.006		.001	.0003
SS_R	0.494	0.024	0.481	0.036	0.487	0.028	0.515	0.030	.103	.378	.0005	.031				.0003	.004
UNC_L	0.433	0.055	0.416	0.054	0.433	0.047	0.451	0.057	.219	.913	.069					.032	
UNC_R	0.458	0.055	0.429	0.059	0.446	0.043	0.457	0.041	.709	.335	.034	.015				.076	
Limbic Association																	
CGC_L	0.444	0.032	0.425	0.038	0.426	0.030	0.448	0.036	.954	.980	.0033	.019	.039			.031	.051
CGC_R	0.415	0.036	0.405	0.034	0.398	0.030	0.423	0.038	.851	.405	.0092		.046			.081	.026
CGH_L	0.320	0.039	0.314	0.038	0.317	0.040	0.332	0.038	.698	.809	.038					.08	
CGH_R	0.331	0.030	0.318	0.039	0.327	0.045	0.335	0.033	.751	.459	.044	.03				.097	
FxS_L	0.422	0.035	0.433	0.026	0.417	0.035	0.453	0.037	.531	.002	.021			.018	.052	.037	.001
FxS_R	0.440	0.030	0.429	0.031	0.420	0.040	0.445	0.043	.558	.483	.0042	.08	.015				.02
Commissural																	
BCC	0.531	0.052	0.518	0.045	0.508	0.050	0.521	0.035	.165	.768	.072		.025				
GCC	0.586	0.046	0.571	0.035	0.575	0.032	0.582	0.031	.685	.413	.045	.026					
SCC	0.722	0.023	0.711	0.028	0.719	0.019	0.719	0.028	.823	.239	.188	.05					
Projection																	
ALIC_L	0.531	0.038	0.511	0.036	0.521	0.028	0.555	0.020	.047	.491	.00002	.003	.076	.085		.00001	.001
ALIC_R	0.546	0.040	0.519	0.031	0.536	0.035	0.559	0.024	.084	.556	.0002	.001			.067	.0001	.032
PLIC_L	0.657	0.036	0.647	0.029	0.663	0.024	0.661	0.022	.215	.230	.315	.083			.055		
PLIC_R	0.658	0.036	0.649	0.022	0.664	0.016	0.657	0.026	.262	.133	.690				.041		
ACR_L	0.396	0.028	0.381	0.031	0.382	0.028	0.406	0.021	.684	.685	.00006	.003	.008			.001	.003
ACR_R	0.411	0.034	0.387	0.037	0.396	0.035	0.421	0.026	.412	.782	.00009	.001	.021			.001	.014
PCR_L	0.421	0.036	0.402	0.028	0.416	0.033	0.430	0.031	.192	.567	.007	.01				.005	
PCR_R	0.425	0.037	0.416	0.024	0.425	0.031	0.436	0.028	.213	.961	.041	.097				.021	
SCR_L	0.431	0.031	0.415	0.033	0.433	0.025	0.437	0.022	.136	.212	.0245	.006			.032	.009	
SCR_R	0.424	0.036	0.409	0.030	0.422	0.024	0.424	0.021	.540	.172	.037	.007				.056	

Note: Values in **bold italics** exceed the false discovery rate (FDR) threshold for significance; other values $p < .05$ did not meet the FDR threshold; empty cell = not significant, $p > .1$; LR = Low Risk; HR = High Risk; LPA = Low Physical Activity; HPA = High Physical Activity; ACR = anterior corona radiate; ALIC = anterior limb of internal capsule; BCC = body of corpus callosum; CGC = cingulum (cingulate gyrus); CGH = cingulum - hippocampal projection; FxS = fornix (cres)/Stria terminalis; GCC = genu of corpus callosum; PCR = posterior corona radiate; PLIC = posterior limb of internal capsule; SCC = splenium of corpus callosum; SCR = superior corona radiate; SLF = superior longitudinal fasciculus; SS = sagittal stratum (includes inferior longitudinal fasciculus and inferior fronto-occipital fasciculus); UNC = uncinata fasciculus.

Supplemental Table 2. Mean and standard deviation (SD) values (mm²/sec) for mean diffusivity (MD) in the four groups of participants within the 25 white matter (WM) fiber tracts.

WM Tract	Low Risk - High PA		Low Risk - Low PA		High Risk - High PA		High Risk - Low PA		Risk	PA	Risk * PA	LR-HPA vs. LR-LPA	LR-HPA vs. HR-HPA	LR-HPA vs. HR-LPA	LR-LPA vs. HR-HPA	LR-LPA vs. HR-LPA	HR-HPA vs. HR-LPA
	Mean	SD	Mean	SD	Mean	SD	Mean	SD	p-value	p-value	p-value						
Long Association																	
SLF_L	0.763	0.033	0.780	0.036	0.763	0.034	0.742	0.026	.031	.989	.0013	.01			.091	.00017	.034
SLF_R	0.764	0.034	0.779	0.035	0.770	0.035	0.750	0.027	.241	.935	.0020	.012				.003	.046
SS_L	0.850	0.037	0.863	0.039	0.871	0.052	0.837	0.034	.973	.34	.0027	.091	.029			.032	.01
SS_R	0.835	0.040	0.849	0.039	0.857	0.047	0.825	0.035	.884	.418	.0036	.086	.028			.047	.015
UNC_L	0.827	0.046	0.848	0.052	0.849	0.037	0.840	0.043	.362	.426	.070	.041	.054				
UNC_R	0.830	0.042	0.844	0.051	0.833	0.028	0.835	0.030	.951	.218	.168	.043					
Limbic Association																	
CGC_L	0.762	0.030	0.774	0.031	0.767	0.034	0.751	0.027	.303	.959	.0130	.051				.013	.096
CGC_R	0.761	0.035	0.775	0.033	0.761	0.025	0.745	0.028	.073	.918	.0096	.031				.002	
CGH_L	0.830	0.055	0.833	0.052	0.857	0.047	0.847	0.068	.048	.917	.340		.039		.099		
CGH_R	0.831	0.042	0.823	0.038	0.849	0.044	0.822	0.026	.189	.064	.095		.036		.013		.023
FxS_L	0.967	0.094	0.942	0.053	0.964	0.086	0.915	0.070	.712	.043	.132						.023
FxS_R	0.985	0.140	0.989	0.099	1.027	0.133	0.967	0.117	.331	.433	.041		.034				.067
Commissural																	
BCC	0.961	0.069	0.984	0.057	0.967	0.071	0.968	0.071	.83	.199	.105	.023					
GCC	0.963	0.063	0.967	0.059	0.969	0.064	0.970	0.040	.355	.606	.404						
SCC	0.804	0.033	0.826	0.041	0.809	0.046	0.802	0.037	.465	.311	.040	.016				.049	
Projection																	
ALIC_L	0.807	0.054	0.834	0.067	0.793	0.049	0.773	0.049	.01	.546	.0138	.015			.012	.00046	
ALIC_R	0.789	0.048	0.815	0.049	0.775	0.040	0.770	0.042	.009	.196	.041	.009			.003	.001	
PLIC_L	0.700	0.025	0.711	0.024	0.696	0.025	0.689	0.020	.032	.546	.038	.035			.031	.003	
PLIC_R	0.698	0.022	0.709	0.024	0.698	0.022	0.697	0.019	.228	.275	.184	.06			.072	.075	
ACR_L	0.869	0.065	0.868	0.049	0.876	0.048	0.840	0.034	.556	.169	.0218				.041	.018	
ACR_R	0.841	0.054	0.850	0.053	0.850	0.043	0.825	0.045	.831	.662	.0199				.07	.072	
PCR_L	0.863	0.066	0.891	0.075	0.846	0.051	0.826	0.060	.013	.638	.038	.043			.021	.0014	
PCR_R	0.863	0.054	0.885	0.057	0.848	0.059	0.820	0.044	.003	.99	.0136	.049		.052	.021	.00017	
SCR_L	0.759	0.034	0.777	0.036	0.755	0.028	0.736	0.026	.005	.785	.0006	.003		.093	.015	.000014	.035
SCR_R	0.753	0.028	0.767	0.028	0.758	0.036	0.733	0.022	.061	.626	.0003	.011				.00012	.007

Note: Values in **bold italics** exceed the false discovery rate (FDR) threshold for significance; other values $p < .05$ did not meet the FDR threshold; empty cell = not significant, $p > .1$; LR = Low Risk; HR = High Risk; LPA = Low Physical Activity; HPA = High Physical Activity; ACR = anterior corona radiate; ALIC = anterior limb of internal capsule; BCC = body of corpus callosum; CGC = cingulum (cingulate gyrus); CGH = cingulum - hippocampal projection; FxS = fornix (cres)/Stria terminalis; GCC = genu of corpus callosum; PCR = posterior corona radiate; PLIC = posterior limb of internal capsule; SCC = splenium of corpus callosum; SCR = superior corona radiate; SLF = superior longitudinal fasciculus; SS = sagittal stratum (includes inferior longitudinal fasciculus and inferior fronto-occipital fasciculus); UNC = uncinata fasciculus.

Supplemental Table 3. Mean and standard deviation (SD) values (mm²/sec) for axial diffusivity (DA) in the four groups of participants within the 25 white matter (WM) fiber tracts.

WM Tract	Low Risk - High PA		Low Risk - Low PA		High Risk - High PA		High Risk - Low PA		Risk	PA	Risk * PA	LR-HPA vs. LR-LPA	LR-HPA vs. HR-HPA	LR-HPA vs. HR-LPA	LR-LPA vs. HR-HPA	LR-LPA vs. HR-LPA	HR-HPA vs. HR-LPA
	Mean	SD	Mean	SD	Mean	SD	Mean	SD	p-value	p-value	p-value						
Long Association																	
SLF_L	1.151	0.041	1.164	0.045	1.151	0.048	1.135	0.040	.218	.96	.074					.033	
SLF_R	1.143	0.040	1.159	0.046	1.152	0.051	1.129	0.039	.468	.898	.018	.072			.028	.102	
SS_L	1.339	0.053	1.345	0.053	1.349	0.059	1.340	0.041	.842	.883	.566						
SS_R	1.330	0.060	1.343	0.060	1.354	0.064	1.344	0.055	.337	.868	.370						
UNC_L	1.248	0.082	1.262	0.070	1.284	0.078	1.290	0.053	.057	.537	.787						
UNC_R	1.287	0.087	1.290	0.077	1.277	0.061	1.292	0.053	.996	.496	.933						
Limbic Association																	
CGC_L	1.151	0.055	1.147	0.063	1.134	0.054	1.136	0.062	.351	.999	.908						
CGC_R	1.111	0.057	1.120	0.052	1.088	0.053	1.092	0.049	.054	.507	.659				.041	.094	
CGH_L	1.132	0.071	1.131	0.067	1.169	0.063	1.165	0.069	.023	.900	.919		.091		.056		
CGH_R	1.147	0.056	1.121	0.048	1.164	0.047	1.141	0.046	.112	.031	.874	.069			.004		
FxS_L	1.408	0.114	1.386	0.069	1.395	0.087	1.377	0.083	.878	.436	.622						
FxS_R	1.446	0.146	1.443	0.124	1.490	0.140	1.440	0.129	.217	.538	.128		.053				
Commissural																	
BCC	1.621	0.058	1.639	0.065	1.596	0.064	1.613	0.082	.168	.153	.593				.027		
GCC	1.730	0.064	1.693	0.072	1.709	0.064	1.721	0.045	.587	.518	.206						
SCC	1.651	0.056	1.673	0.061	1.659	0.074	1.640	0.062	.487	.803	.088						
Projection																	
ALIC_L	1.342	0.052	1.358	0.076	1.309	0.059	1.319	0.063	.028	.234	.457				.008	.038	
ALIC_R	1.334	0.046	1.344	0.059	1.317	0.061	1.321	0.060	.17	.463	.576				.097		
PLIC_L	1.320	0.041	1.330	0.038	1.322	0.040	1.305	0.022	.225	.728	.077					.036	
PLIC_R	1.318	0.037	1.329	0.045	1.327	0.049	1.314	0.020	.752	.956	.197						
ACR_L	1.267	0.058	1.261	0.051	1.268	0.048	1.246	0.036	.822	.292	.215						
ACR_R	1.252	0.056	1.238	0.050	1.249	0.032	1.241	0.047	.728	.38	.852						
PCR_L	1.292	0.080	1.311	0.090	1.273	0.072	1.247	0.086	.045	.969	.132					.013	
PCR_R	1.297	0.071	1.316	0.079	1.285	0.081	1.245	0.064	.025	.632	.048		.075		.003		
SCR_L	1.145	0.054	1.151	0.043	1.144	0.047	1.117	0.040	.16	.379	.053				.018	.07	
SCR_R	1.130	0.050	1.138	0.039	1.137	0.053	1.101	0.027	.184	.172	.017			.083	.009	.016	

Note: Values in **bold italics** exceed the false discovery rate (FDR) threshold for significance; other values $p < .05$ did not meet the FDR threshold; empty cell = not significant, $p > .1$; LR = Low Risk; HR = High Risk; LPA = Low Physical Activity; HPA = High Physical Activity; ACR = anterior corona radiate; ALIC = anterior limb of internal capsule; BCC = body of corpus callosum; CGC = cingulum (cingulate gyrus); CGH = cingulum - hippocampal projection; FxS = fornix (cres)/Stria terminalis; GCC = genu of corpus callosum; PCR = posterior corona radiate; PLIC = posterior limb of internal capsule; SCC = splenium of corpus callosum; SCR = superior corona radiate; SLF = superior longitudinal fasciculus; SS = sagittal stratum (includes inferior longitudinal fasciculus and inferior fronto-occipital fasciculus); UNC = uncinata fasciculus.

Supplemental Table 4. Mean and standard deviation (SD) values (mm²/sec) for radial diffusivity (DR) in the four groups of participants within the 25 white matter (WM) fiber tracts.

WM Tract	Low Risk - High PA		Low Risk - Low PA		High Risk - High PA		High Risk - Low PA		Risk	PA	Risk * PA	LR-HPA vs. LR-LPA	LR-HPA vs. HR-HPA	LR-HPA vs. HR-LPA	LR-LPA vs. HR-HPA	LR-LPA vs. HR-LPA	HR-HPA vs. HR-LPA
	Mean	SD	Mean	SD	Mean	SD	Mean	SD	p-value	p-value	p-value						
Long Association																	
SLF_L	0.570	0.037	0.588	0.038	0.569	0.032	0.546	0.027	.021	.957	.0005	.0054			.074	.000053	.02
SLF_R	0.574	0.038	0.591	0.038	0.579	0.031	0.561	0.027	.201	.75	.0025	.0079				.002	.07
SS_L	0.606	0.038	0.623	0.044	0.632	0.056	0.585	0.038	.937	.202	.0001	.028	.006			.004	.001
SS_R	0.588	0.037	0.609	0.051	0.608	0.046	0.565	0.038	.404	.369	.0003	.025	.04			.002	.003
UNC_L	0.617	0.056	0.641	0.066	0.631	0.045	0.615	0.066	.88	.586	.0499	.049					
UNC_R	0.602	0.051	0.626	0.063	0.611	0.040	0.606	0.043	.93	.236	.0538	.016					
Limbic Association																	
CGC_L	0.568	0.031	0.588	0.036	0.583	0.035	0.558	0.032	.572	.945	.0006	.006	.035			.004	.02
CGC_R	0.586	0.038	0.602	0.038	0.597	0.027	0.572	0.039	.388	.709	.0026	.032				.006	.026
CGH_L	0.679	0.058	0.684	0.055	0.702	0.052	0.688	0.075	.143	.942	.188		.05				
CGH_R	0.673	0.043	0.674	0.044	0.692	0.059	0.662	0.033	.439	.252	.0255		.033				.029
FxS_L	0.746	0.093	0.719	0.054	0.749	0.091	0.685	0.073	.651	.012	.055			.056		.092	.005
FxS_R	0.727	0.067	0.761	0.093	0.796	0.132	0.730	0.115	.164	.665	.0026	.037	.002				.024
Commissural																	
BCC	0.631	0.088	0.657	0.072	0.653	0.087	0.646	0.075	.388	.35	.083	.036					
GCC	0.583	0.076	0.603	0.065	0.600	0.068	0.595	0.051	.403	.371	.104	.049	.084				
SCC	0.380	0.033	0.402	0.043	0.385	0.037	0.383	0.040	.587	.182	.082	.016					
Projection																	
ALIC_L	0.540	0.060	0.572	0.067	0.535	0.048	0.501	0.044	.010	.827	.0013	.0061			.0254	.00006	.047
ALIC_R	0.516	0.055	0.551	0.049	0.509	0.042	0.494	0.039	.007	.226	.0051	.0017			.0024	.00013	
PLIC_L	0.390	0.037	0.405	0.033	0.382	0.027	0.381	0.025	.059	.235	.099	.026			.016	.013	
PLIC_R	0.389	0.035	0.404	0.031	0.383	0.016	0.388	0.028	.153	.087	.279	.029			.014	.077	
ACR_L	0.666	0.065	0.674	0.053	0.680	0.051	0.636	0.036	.553	.226	.0030		.082			.011	.0067
ACR_R	0.636	0.058	0.650	0.051	0.651	0.053	0.617	0.048	.756	.646	.0043	.053	.065			.024	.03
PCR_L	0.649	0.066	0.681	0.070	0.633	0.047	0.615	0.055	.01	.437	.0222	.0155			.00086	.00065	
PCR_R	0.646	0.055	0.670	0.052	0.630	0.052	0.607	0.043	.002	.733	.0117	.023		.07	.0074	.0001	
SCR_L	0.566	0.034	0.591	0.041	0.560	0.027	0.545	0.026	.003	.299	.0004	.0003			.0017	.000062	.09
SCR_R	0.564	0.033	0.583	0.034	0.568	0.034	0.549	0.025	.079	.643	.0004	.0014			.08	.00021	.037

Note: Values in **bold italics** exceed the false discovery rate (FDR) threshold for significance; other values $p < .05$ did not meet the FDR threshold; ns = not significant; LR = Low Risk; HR = High Risk; LPA = Low Physical Activity; HPA = High Physical Activity; ACR = anterior corona radiate; ALIC = anterior limb of internal capsule; BCC = body of corpus callosum; CGC = cingulum (cingulate gyrus); CGH = cingulum - hippocampal projection; FxS = fornix (cres)/Stria terminalis; GCC = genu of corpus callosum; PCR = posterior corona radiate; PLIC = posterior limb of internal capsule; SCC = splenium of corpus callosum; SCR = superior corona radiate; SLF = superior longitudinal fasciculus; SS = sagittal stratum (includes inferior longitudinal fasciculus and inferior fronto-occipital fasciculus); UNC = uncinata fasciculus.